Stopping power of Al, Cu, Ag, and Au for MeV hydrogen, helium, and lithium ions. Z_1^3 and Z_1^4 proportional deviations from the Bethe formula

H. H. Andersen, J. F. Bak, H. Knudsen, and B. R. Nielsen
Institute of Physics, University of Aarhus, DK-8000 Aarhus C, Denmark
(Received 16 June 1977)

Stopping power of Al, Cu, Ag, and Au for 0.8–7.2-MeV/amu hydrogen, helium, and lithium ions has been measured by the calorimetric-compensation method to an accuracy of 0.5%. The data agree with most other published results and confirm the validity of earlier measurements by Andersen and co-workers. Higher-order Z_1 deviations from the Bethe formula have been examined. The experimental results agree with Lindhard's calculation of the Z_1^3 correction combined with a Z_1^4 term, which is slightly larger than Bloch's value. The experimental higher-order Z_1 contributions have a significant influence on the evaluation of empirical shell corrections, and the data are used to extract more realistic values. The deduced shell corrections show good agreement with Bonderup's calculations.

I. INTRODUCTION

Some years ago, comprehensive measurements of stopping powers of a number of elements for protons, deuterons, and α particles in the MeV range were carried out by Andersen and co-workers at Risö[1–6](in the following referred to as the Risö measurements). These measurements were performed by means of the calorimetric-compensation technique, and absolute stopping powers were obtained with a standard deviation of 0.4%,[7] thereby complying with both theoretical and experimental demands for more accurate stopping-power data. Since the Risö data comprise a relatively large fraction of existing high-accuracy stopping-power data, they will significantly influence empirical tabulations.[8] As some measurements, claimed to be of comparable accuracy, were found to be at variance with the Risö data,[9–11] we decided to check these data at another accelerator facility.

Another purpose was to investigate the energy dependence of stopping powers at lower energies (down to 0.8 MeV/amu) in order to obtain information on the shell corrections to the Bethe formula also in this energy range (cf. Sec. II). Furthermore, we included measurements of stopping powers for lithium ions in order to perform a more detailed investigation of the observed deviations from the theoretical projectile-charge dependence of the stopping power.[6] A brief report on the above aspect of the present work has been published recently.[12] The deviations will be shown to have a great influence on empirical shell corrections deduced from experimental data.

II. THEORY

The theory of energy loss of fast, charged particles in matter is based on the calculations by Bethe.[13,14] The result for the stopping power of a target of atomic number Z_2 and mass number A for a projectile of charge Z_1e and velocity v is

$$-\frac{dE}{dx}=\frac{4\pi e^4 N_0 Z_2}{mv^2 A}Z_1^2 L_0(v,Z_2)\,, \tag{1}$$

where

$$L_0(v,Z_2)=\ln\left(\frac{2mv^2}{I}\right)+\ln\left(\frac{1}{1-\beta^2}\right)-\beta^2-\frac{C}{Z_2}\,. \tag{2}$$

Here $-e$ and m are the electron charge and mass, respectively, N_0 is Avogadro's number, β is the ratio of the projectile velocity to the speed of light. I and C/Z_2 are the target mean-excitation potential and the shell corrections, respectively. They are the main, nontrivial, parameters of the theory and have been subject to substantial theoretical work.[15] The mean-excitation potential is defined as

$$\ln I=\sum_n f_n \ln E_n \tag{3}$$

where E_n are all possible energy transitions of the target atom and f_n are the corresponding dipole-oscillator strengths. In practice, attempts to calculate I are usually based on a statistical model of the target atom. As their most simple result, such calculations yield Bloch's rule, i.e., $I=I_0Z_2$, with $I_0\simeq 10$ eV. The shell corrections are an integral part of the Bethe stopping theory. They are of importance when the velocities of the bound target electrons are not negligible as compared to the projectile velocity. Calculations for K- and L-shell electrons were carried out by Walske as described in detail in Fano's review article,[14] but more convenient results emerge from a treatment based on the statistical-atomic model. Bonderup[16] used the theoretically known stopping power of a free-electron gas and assumed that this result

could be used even for an inhomogenous electron distribution. With this assumption, total stopping powers were obtained by integration over the Thomas-Fermi electron-density distributions for target atoms. From the calculated stopping powers, shell corrections were finally deduced.

Bethe's calculation is based on first-order quantal perturbation theory, which is the reason for the stopping-power expression to come out proportional to Z_1^2. Thus Eq. (1) is an asymptotic expression, which is valid for $\kappa \ll 1$ only, where $\kappa = 2Z_1 v_0/v$, v_0 being the Bohr velocity ($v_0 = e^2/\hbar$). Nevertheless, the formula is well known to fit experimental data to a relatively high accuracy even at fairly low projectile velocities. A more universal stopping-power formula was obtained by Bloch[17] in a calculation valid for all values of κ, the only restriction being that the projectile velocity must not be too low compared to the velocities of target electrons. Bloch found an expression similar to Eq. (1) but with $\ln(2mv^2/I)$ replaced by

$$\ln(2mv^2/I) + \psi(1) - \mathrm{Re}\psi(1 + i\kappa/2) , \tag{4}$$

where ψ is the logarithmic derivative of the Γ function. For small κ, we retrieve Bethe's expression. In fact, Eq. (4) is equal to $\ln(2mv^2/I)$ to within 1% for values of $\kappa \lesssim 0.3$. At higher values of κ, the Bloch expression differs from Eq. (2) in the dependence on both projectile charge and velocity. The high-κ limit of (4) is

$$\ln\left(\frac{2mv^2}{I}\frac{1.123}{\kappa}\right) , \tag{5}$$

which is the result of the classical impact-parameter calculation by Bohr,[18,19] whose treatment should be valid for $\kappa \gg 1$. Bloch's calculation thus concerns the correspondence between the classical and the quantal description of the interaction. For values of κ smaller than 1, the following approximation, which includes the leading term in an expansion of (4) in $\kappa/2$, is valid to within a few percent,

$$Z_1^2 L_2 \equiv L_{\mathrm{Bloch}} - L_0 \simeq -1.202(\kappa/2)^2 . \tag{6}$$

Since κ is proportional to Z_1, this gives a correction to the Bethe formula, which is proportional to Z_1^4. Higher-order terms in this expansion are all proportional to even powers of $\kappa/2$, and the numerical factors are close to 1.

Due to certain experimental evidence[6,20,21] throughout the last few years, further theoretical efforts[22–27] have been devoted to revealing the deficiencies of the Bethe formula, which are present because the calculation is based on the first-order Born approximation. Using a semiclassical treatment, Ashley *et al.*[22] found a corrective term to the Bethe formula proportional to Z_1^3. With a suitable choice of lower-impact-parameter cut-off, Jackson and McCarthy[23] found a scaling of this term, which may be expressed in the following way,

$$Z_1 L_1 \equiv L_{J,M} - L_0 = Z_1 \frac{F((v/v_0)Z_2^{-1/2})}{Z_2^{1/2}} L_0 , \tag{7}$$

where F is a universal function of the reduced velocity $(v/v_0)Z_2^{-1/2}$. This result deviates very little from the result of Ashley *et al.*[24] Further, Hill and Merzbacher[25] have shown that the result of an equivalent quantal calculation is equal to Eq. (7). Lindhard[26] and Esbensen[27] used a different approach, calculating the stopping by a free-electron gas and by harmonically bound electrons. The results suggest Eq. (7) to be too small by approximately a factor of 2, which is due to the fact that the calculations of the previous authors do not include a contribution from close collisions with target electrons.

Considering the above corrections to the Bethe formula, we may write the following, more detailed, expression,

$$-\frac{dE}{dx} = \frac{4\pi e^4 N_0 Z_2}{mv^2 A} Z_1^2 [L_0 + Z_1 L_1 + Z_1^2 L_2] . \tag{8}$$

Because of still higher-order approximations, the exact stopping-power formula will contain an infinite number of terms within the brackets.

The existence of the correction terms in Eq. (8) has important implications for the evaluation of shell corrections and mean-excitation potentials from experimental stopping-power data. Although a theoretical Z_1^3 term has recently been taken into account by Ashley,[28] the Z_1^4 term has not been included in such evaluations previously.

III. EXPERIMENTAL METHOD AND DATA TREATMENT

The calorimetric-compensation technique, which has been described in detail elsewhere,[1,29] has been used. Only a brief outline of the technique will be given here. The principle is shown in Fig. 1. The ion beam passes through the target foil and is stopped in a box-shaped beam stop (the block). Foil and block are both connected to a liquid-helium cryostat through thermal resistances W_F and W_B, respectively. The energy lost by the projectiles is converted into heat, resulting in temperature rises of both systems, which are continuously measured by means of the resistance thermometers R_F and R_B. After irradiation, the power dissipated by the beam in the foil and the block is compensated for by known powers deposited in two electrical heaters thermally connected to the systems. The very low working temperature

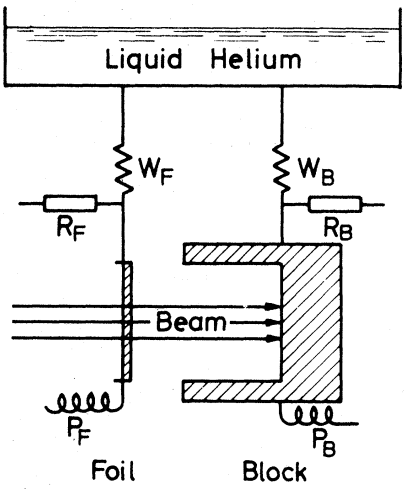

FIG. 1. Schematic drawing of the calorimetry systems. W_F and W_B are the thermal resistances connecting the foil and block to the liquid-helium reservoir. R_F and R_B are resistance thermometers and P_F and P_B are the electrical heaters connected to the foil and block, respectively.

ensures high thermal conductivities and thereby also a constant temperature throughout each of the systems. In addition, thermal radiation loss is negligible. Therefore, if P_F and P_B are the electrical powers necessary to obtain the same temperature rises of the foil and block thermometers as those measured during irradiation, the relative energy loss of the projectiles is given by

$$\Delta E/E_0 = P_F/(P_F+P_B), \tag{9}$$

where E_0 is the energy of the impinging projectiles. Knowing the target thickness t and the beam energy, we have the stopping power as

$$\left(-\frac{dE}{dx}\right)_{E=E'} = \frac{P_F}{P_F+P_B}\frac{E_0}{t}, \tag{10}$$

where the stopping power is attributed to the mean particle energy within the foil, i.e., $E'=E_0-\Delta E/2$. The error in the stopping power due to this approximation does not exceed 0.05% when the relative energy loss is less than 20%,[1] which was always the case in the present work. The error was thus neglected.

So far, our description of the measuring technique has been based on the assumption that all the energy lost by the projectiles appears as heat within the foil and block. Small corrections have been calculated for protons and deuterons in Refs. 1 and 29. Extending these calculations to include helium and lithium ions, for the energy range covered here we still find that corrections for stored energy, sputtering, low-energy secondary electrons, and nuclear reactions are of no significance. On the other hand, in most cases, the corrections for energy escaping as x rays and δ rays from the foil are non-negligible, and the data were corrected acccrding to formulas analogous to those of Ref. 1. The δ-ray correction used has been further discussed in Ref. 7 and was found to be slightly overestimated, which is also concluded from a comparison of the calculated corrections with the experimental data of Ref. 30 for δ rays escaping from a carbon foil. However, at the relatively low velocities considered here, the correction is small, and the error introduced should be of no significance. Furthermore, Eq. (10) assumes the projectile paths to be straight lines. The data were therefore corrected for multiple and single scattering. The total uncertainty in the corrections is estimated to be ~0.1% of the stopping power.

Our measuring equipment is a rebuilt version of that described in detail in Refs. 1 and 29. In order to facilitate the data treatment, each thermometry system has been connected to a linear-integration system. This system was used both during the actual runs and during the subsequent power calibrations. Hence, power ratios in Eq. (9) were obtained directly with no need for tracing out the detailed temperature fluctuations during runs. However, for a number of runs, power ratios were evaluated also from the recorded fluctuating temperatures by the procedure described in Ref. 1, which yielded identical results. The uncertainty in the measurement of the power ratio was found to be ~0.1% as long as the beam fluctuations were less than $\pm 10\%$, which was the case in the present measurements.

The ion beam was obtained from the Aarhus HVEC type-EN tandem Van de Graaff accelerator. In the hydrogen and helium runs, a duoplasmatron ion source with charge exchange was used, while the lithium ions were produced by a sputtering ion source.[31] The beam energy was determined from the field of the analyzing magnet. Prior to entering the foil, the beam was swept homogeneously over a large area of the target (6.5×13.0 mm) by horizontal and vertical high-frequency deflection systems.

Since the uncertainty due to the energy measurement constitutes the major part of the total uncertainty, we performed a comprehensive differential energy calibration of the analyzing magnet.[32] The shape of the calibration curve was traced by consecutive transmission of different ions or ions of different charge states through the accelerator and the analyzing magnet. Since the acceleration voltage was kept constant during each run, ratios between projectile energies were known, and by a comparison of these with the magnetic-field ratios,

we acquired information as to the shape of the calibration curve. By the use of several different acceleration voltages, the total amount of data points made it possible to trace out the entire curve. It was concluded that the standard deviation of the energy measurement was 0.15%. Since the stopping power is roughly inversely proportional to the energy, it is seen from Eq. (10) that the relative standard deviation in the measured stopping powers originating from the uncertainty on the energy is twice the latter, i.e., 0.3%.

In Eq. (9), the beam was assumed to be monoenergetic. However, due to inevitable slit scattering during the beam transport, the beam contains some low-energy ions which, if sufficiently numerous, may lead to experimental stopping-power values which are too high. We therefore analyzed the energy spectra of several beams at different energies by means of standard Rutherford-scattering techniques.[33] Because of scattering at the edges of the detector apertures, only an upper limit to the influence of slit-scattered particles could be obtained. This limit was estimated to be 0.2%, which should be included in the total uncertainty.

The target thickness was determined as the weight/area of the irradiated part of the foil, which was cut out by means of a punching tool of the same size as the beam-defining aperture. The measured thickness was corrected for thermal contraction during cooling-down. The standard deviation of the thickness determination was 0.2%. The homogeneous irradiation of the part of the foil cut out afterwards ensures that the influence of even large thickness variations is negligible.

The resulting standard deviation of the stopping-power values, including all the above uncertainties, is concluded to be 0.5%.

IV. RESULTS AND DISCUSSION

A. Stopping power

The present investigation includes measurements of stopping powers for hydrogen, helium, and lithium ions in the energy range from 0.8 to 7.2 MeV/amu. The target materials used were rolled foils of Al, Cu, Ag, and Au, manufactured by Goodfellows Metals Ltd. Target thicknesses varied from 1 to 6 mg/cm^2, and the claimed purities were 99.5% for the Al foils and 99.9% for the other materials.

The data are presented as reduced stopping powers,[34] defined by

$$X \equiv f(\beta) - \left(-\frac{dE}{dx}\right)\frac{mv^2 A}{4\pi N_0 e^4 Z_2 Z_1^2}, \tag{11}$$

where

$$f(\beta) \equiv \ln\left(\frac{2mv^2}{1-\beta^2}\right) - \beta^2. \tag{12}$$

Since X varies slowly over the energy range investigated here, this way of presentation has the virtue of revealing small differences in the measured stopping powers. For the sake of clarity, the data for protons and deuterons are shown in Figs. 2–5 as experimental curves drawn by eye through the considerable amount of data points (in total, more than 450 data points were measured). Comparisons are made to existing experimental data of accuracies better than ±2.5% and to the

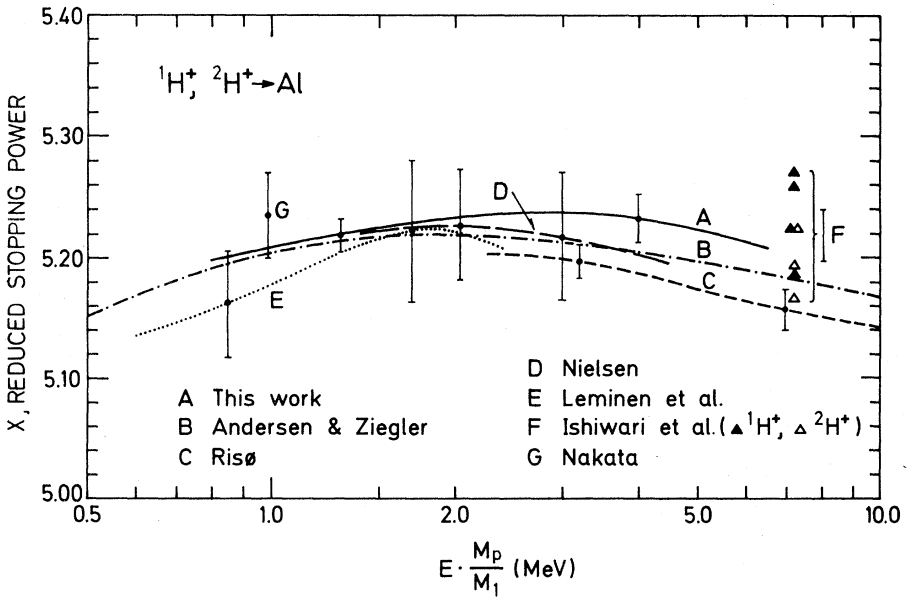

FIG. 2. Experimental reduced stopping powers for H ions in Al as a function of the equivalent proton energy, EM_P/M_1. Curve A is drawn by hand through all the data points. Curve B is the empirical tabulations of Ref. 8. Experimental data from Refs. 5 and 35–37 are labeled C, D, E, and G, respectively. Data points F are from Refs. 9–11. Representative error bars are shown.

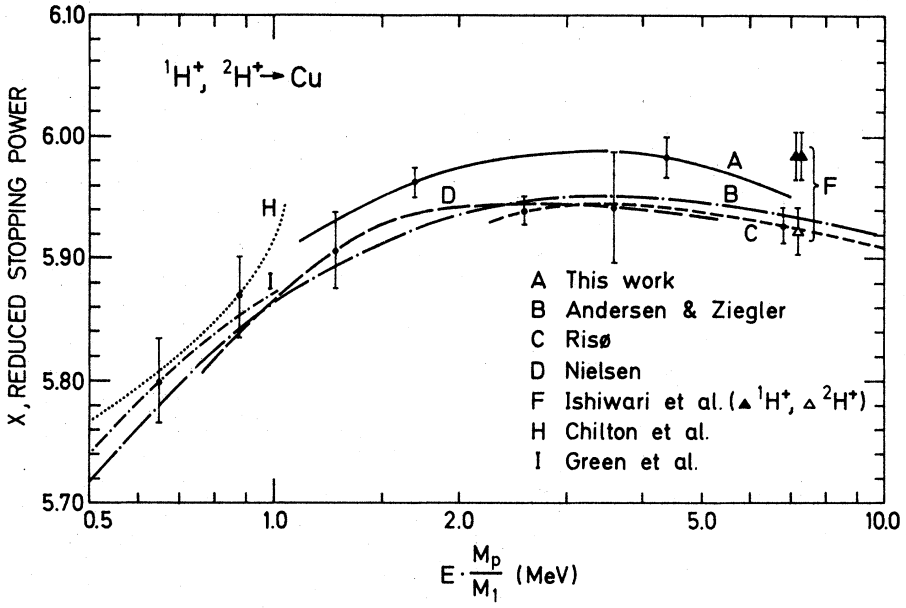

FIG. 3. Experimental reduced stopping powers for H in Cu. Data groups B, C, D, H, and I are from Refs. 8, 5, 35, 38, and 39, respectively. Data points F are from Refs. 9–11.

empirical calculations of Andersen and Ziegler,[8] who claim their accuracy to be ±0.5% (standard deviation).

Generally, our data are in good agreement with other data. Exceptions are found for some of the data points of Ishiwari *et al.*[9–11] in aluminum and gold and in part of the data of Nielsen[35] in gold and silver. However, the spread in the data of Refs. 9–11 and the discrepancy between their proton and deuteron stopping powers seem to indicate that their claimed uncertainty is too optimistic.[41] Also, the Risö data and the tabulations of Ref. 8 agree (within two standard deviations) with our data except for the lower-energy data in copper, but relatively few points were measured on this target material. With the exception of the gold data, our stopping powers seem to be systematically lower than the Risö data. (Note: Larger X values mean smaller stopping powers.) This may be due to the uncertainty in the energy calibration in either ours or the Risö measurements since an error in this calibration results in systematic shifts of the data in the entire energy range and for all targets. Also, no upper limit for the possible influence of beam contamination was set for the Risö data. However, the stopping power of gold is found to be

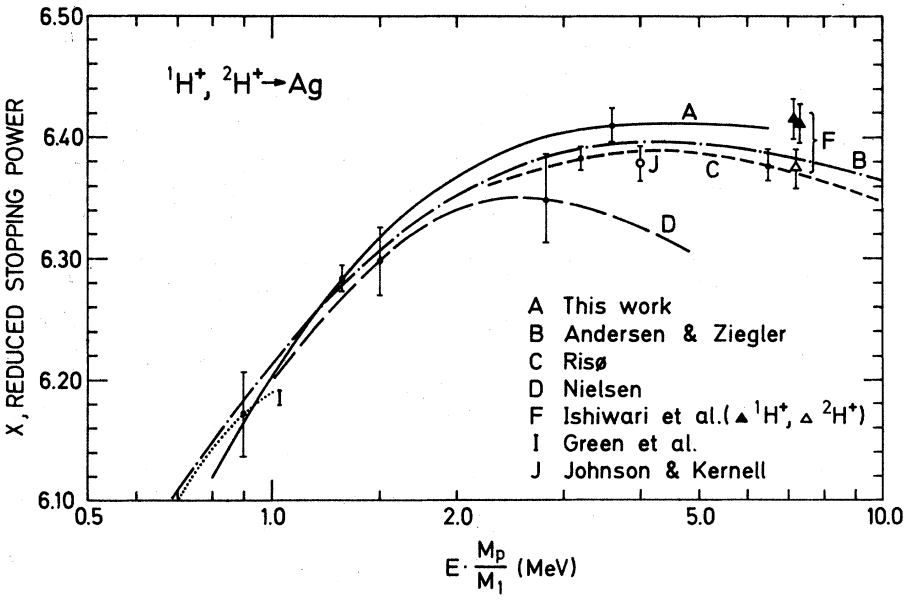

FIG. 4. Experimental reduced stopping powers for H in Ag. Data groups B, C, D, I, and J are from Refs. 8, 5, 35, 39, and 40, respectively. Data points F are from Refs. 9–11.

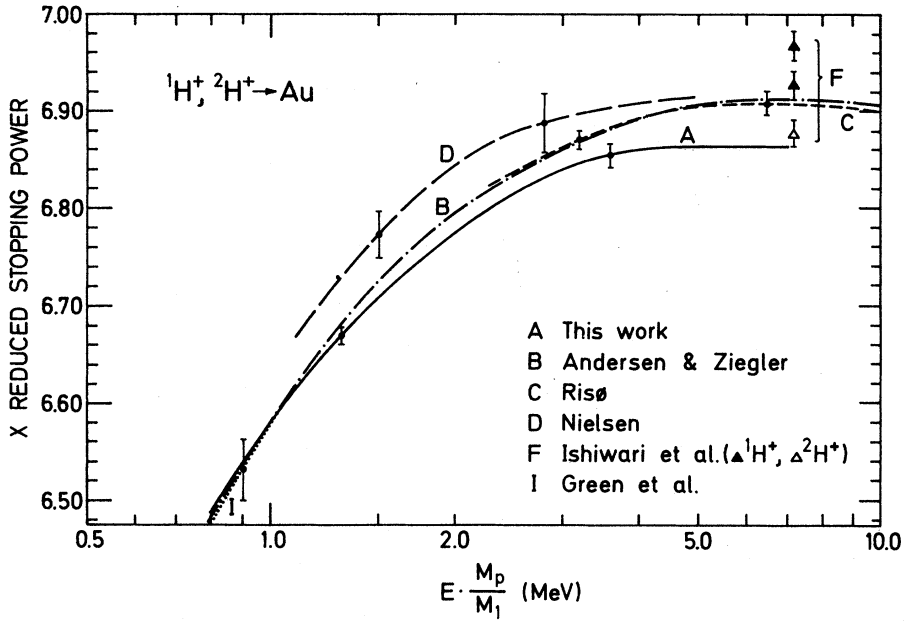

FIG. 5. Experimental reduced stopping powers for H in Au. Data groups B, C, D, and I are from Refs. 8, 5, 35, and 39, respectively. Data points F are from Refs. 9–11.

larger than that measured at Risö. The reason for this is not understood since almost all sources of error should have a similar influence on all the data.

Figure 6 shows an example of the data obtained for all three projectiles on one target foil. In the Bethe treatment, $X = \ln I + C/Z_2$, and consequently reduced stopping powers of the same target material for different projectiles should be equal at equal velocities. This is seen not to be the case, and a detailed discussion of the deviations will be presented in the next section. In order to derive stopping powers for helium and lithium ions, curves were drawn through the total amount of data points for each projectile and target material. In Table I, together with the hydrogen stopping powers, the helium and lithium data are listed as the fractional differences from the measured hydrogen stopping powers times the square of the projectile atomic number at equal velocity,

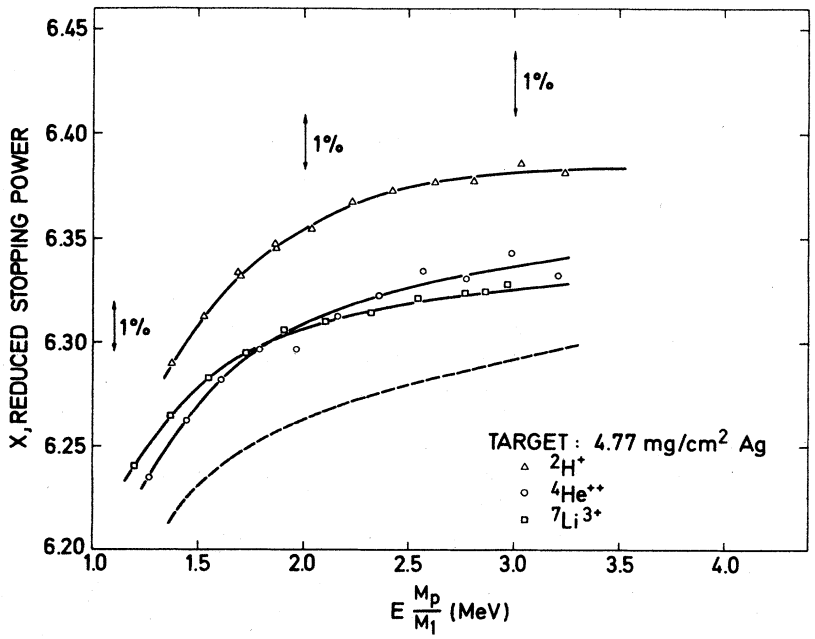

FIG. 6. Experimental reduced stopping powers of Ag for H, He, and Li ions measured in one run. The dotted line is the value of X_{Li} expected from the H and He data in case of no Z_1^4 effect. Arrows indicate the change in X for a 1% change in the stopping power.

TABLE I. Stopping powers of Al, Cu, Ag, and Au for H, He, and Li ions. He and Li values are presented as fractional differences from the tabulated H stopping powers times Z_1^2 [cf. Eq. (13)]. Relative standard deviation on S_H is 0.5%. Absolute standard deviation on Δ_{He} and Δ_{Li} is 0.003. S_H is in units of keV cm^2/mg.

$E(M_p/M_1)$[a] (MeV)	Al			Cu			Ag			Au		
	S_H	Δ_{He}	Δ_{Li}	S_H	Δ_{He}	Δ_{Li}	S_H	Δ_{He}	Δ_{Li}	S_H	Δ_{He}	Δ_{Li}
0.8	196.6	+0.030					105.4	+0.016		70.43		
1.0	172.1	0.025					93.15	0.018		63.53	+0.028	
1.2	153.6	0.021	−0.002	106.6			84.15	0.019	+0.010	58.94	0.025	
1.4	139.0	0.019	+0.006	97.69	+0.021		77.31	0.019	0.015	55.16	0.023	
1.6	127.3	0.017	0.010	90.46	0.019	+0.013	71.69	0.019	0.018	51.91	0.022	+0.024
1.8	117.6	0.015	0.012	84.41	0.018	0.017	67.12	0.019	0.021	49.07	0.021	0.027
2.0	109.5	0.013	0.013	79.29	0.017	0.016	63.26	0.019	0.023	46.64	0.020	0.029
2.2	102.5	0.012	0.014	74.80	0.016	0.015	59.96	0.018	0.024	44.39	0.020	0.029
2.4	96.47	0.011	0.014	70.87	0.015	0.014	57.02	0.018	0.025	42.41	0.019	0.028
2.6	91.19	0.010	0.013	67.38	0.014	0.013	54.41	0.017	0.025	40.63	0.019	0.026
2.8	86.54	0.010	0.013	64.28	0.013	0.012	52.07	0.017	0.024	39.02	0.018	
3.0	82.39	0.009	0.012	61.51	0.013		49.95	0.016	0.023	37.57	0.017	
3.2	78.67	0.008	0.012	58.99	0.012		48.05	0.015		36.27	0.016	
3.4	75.30	0.008	0.011	56.71	0.012		46.32	0.014		35.09	0.014	
3.6	72.26	0.007		54.62	0.011		44.74	0.014		34.00	0.013	
3.8	69.46	0.007		52.71	0.011		43.28	0.013		33.00	0.012	
4.0	66.94	0.006		50.94	0.010		41.92	0.013		32.07	0.010	
4.2	64.61	0.006		49.31	0.010		40.66	0.012		31.21		
4.4	62.46	0.006		47.79	0.010		39.49	0.012		30.41		
4.6	60.47	0.005		46.39	0.009		38.39	0.011		29.65		
4.8	58.61	0.005		45.10	0.009		37.36	0.011		28.93		
5.0	56.88	0.005		43.88	0.009		36.39	0.011		28.26		
5.2	55.26	0.004		42.74			35.49			27.61		
5.4	53.74	0.004		41.67			34.62			27.00		
5.6	52.31	0.003		40.66			33.82			26.42		
5.8	50.97			39.70			33.04			25.87		
6.0	49.70			38.79			32.31			25.34		
6.2	48.50			37.92			31.61			24.84		
6.4	47.37			37.10			30.96			24.36		
6.6				36.31						23.89		
6.8				35.55						23.45		
7.0				34.83						23.03		
7.2				34.13						22.62		

[a] Exact masses must be used to obtain the energy.

$$\Delta_{He}=\frac{S_{He}-4S_H}{S_{He}}, \quad \Delta_{Li}=\frac{S_{Li}-9S_H}{S_{Li}}, \tag{13}$$

where S denotes stopping power. Since a number of uncertainties and corrections cancel in the measurement of stopping-power differences for different ions at equal velocity in the same foil, the absolute standard deviation of Δ_{He} and Δ_{Li} is 0.003 only. If, however, absolute helium or lithium stopping powers are calculated from Table I, these stopping powers will, in turn, be obtained with a relative accuracy of 0.5%. Except for the Risö data[6] and the data of Nakata,[42] both for aluminum, no measurements of helium stopping powers of comparable accuracy (better than 2.5%) are known to exist in the energy range covered. The existing data are all in close agreement with those of Table I. Concerning the lithium data, to the authors' best knowledge no measurements exist in this energy range.

B. Charge dependence of stopping powers

As mentioned above, we observe the X values for hydrogen, helium, and lithium ions at equal velocity to be different, which is inconsistent with the Bethe formula. On the other hand, the deviations may be accounted for by means of the higher-order corrections mentioned in Sec. II. Substitution of Eqs. (2), (8), and (12) into Eq. (11) gives the following formula for the reduced stopping power,

$$X=\ln I+C/Z_2-Z_1L_1-Z_1^2L_2. \tag{14}$$

In case of a negligible Z_1^4 effect (i.e., $L_2\simeq 0$), we obtain $X_H-X_{He}=X_{He}-X_{Li}$. The lithium points

should then lie on the dotted line of Fig. 6, which is apparently not the case, thus indicating a non-zero L_2. More quantitative information on the Z_1^3 and Z_1^4 effects is obtained from solution of Eqs. (8) and (11) for $Z_1 = 1, 2$, and 3, which gives

$$\begin{aligned} L_0 &= f(\beta) - X_{\mathrm{Li}} - 3(X_{\mathrm{H}} - X_{\mathrm{He}}), \\ L_1 &= \tfrac{5}{2}(X_{\mathrm{H}} - X_{\mathrm{He}}) + \tfrac{3}{2}(X_{\mathrm{Li}} - X_{\mathrm{He}}), \\ L_2 &= -\tfrac{1}{2}(X_{\mathrm{H}} - X_{\mathrm{He}}) - \tfrac{1}{2}(X_{\mathrm{Li}} - X_{\mathrm{He}}). \end{aligned} \tag{15}$$

Experimental values of L_0, L_1, and L_2 are found by insertion of the measured reduced stopping powers on the right-hand side of Eqs. (15). The results are shown in Fig. 7 for all targets as a function of v/v_0. In the same figure, comparisons are made to the theoretical expressions for L_1 [Eq. (7)] and L_2 [Eq. (6)]. The uncertainty on the experimental curves are 0.5% for L_0 and approximately 25% for L_1 and L_2. Hence, the detailed shapes of the L_1 and L_2 curves are of no significance, and no conclusions may be drawn from the crossing of curves for different materials. The measured L_1 is seen to be nearly a factor of 2 larger than the theoretical results of Jackson and McCarthy, which supports the estimates of Lindhard.[26] Except for the low-velocity part of the aluminum results, the experimental L_2 values are in agreement with Eq. (6) within the experimental uncertainty although they are all systematically larger than the theoretical value. In the Appendix is shown that the apparent deviations for aluminum are most probably due to electron pick-up by the lithium ions at low energies during their passage through the target. A possible systematic correction to the lithium data will influence the calculation of both L_1 and L_2, as seen from Eqs. (15). Electron pick-up should be of minor significance for heavier targets.

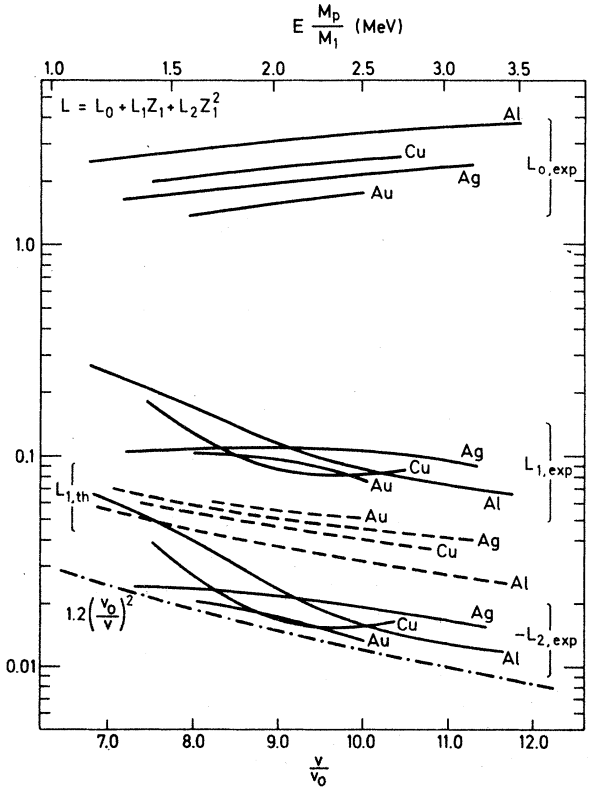

FIG. 7. Experimental curves (fully drawn) for the Bethe logarithm (L_0), the Z_1^3 factor (L_1), and the Z_1^4 factor (L_2) for four target materials. Theoretical curves for L_1 (dashed) and L_2 (dot and dash) are Eqs. (7) and (6), respectively.

A large number of hydrogen-helium stopping-power differences were measured outside the region covered by the lithium measurements. Here, no means of an experimental distinction between Z_1^3 and Z_1^4 contributions is available. However, the information on L_2 from Fig. 7 may be used to extract L_1 from the hydrogen-helium data. A best fit to an average L_2 from data for all targets (excepting the low-velocity part of the aluminum data) is

$$Z_1^2 L_2 = -1.6(\kappa/2)^2 \tag{16}$$

rather than Eq. (6). From Eq. (14), we find

$$L_1 = X_{\mathrm{H}} - X_{\mathrm{He}} - 3L_2. \tag{17}$$

Using experimental data for $X_{\mathrm{H}} - X_{\mathrm{He}}$ and the empirical relation, Eq. (16), for L_2, we thus obtain experimental L_1 values which may be used to test the scaling of Eq. (7) derived by Jackson and McCarthy. In a plot of $Z_2^{1/2} L_1/L_0$ versus $(v/v_0)Z_2^{-1/2}$, the scaling approximately works, but the data for individual target materials were found systematically to be shifted against lower values at constant reduced velocity for increasing Z_2. For example, in the region of overlap, the aluminum values are approximately twice those of gold. Hence we tried empirically to find a scaling. The most favorable result is shown in Fig. 8, where $Z_2^{1/2} L_1/L_0$ is plotted as a function of the reduced velocity $(v/v_0)Z_2^{-1/3}$. The power of Z_2 in this reduced velocity was found to be one-third to within an accuracy of 0.05.

The curve of Fig. 8 represents the equation

$$\Phi(V) = 2.68 V^{-2}(1 - 0.264 \ln V) \tag{18}$$

where

$$V = (v/v_0)Z_2^{-1/3}. \tag{19}$$

The curve is seen to fit the data of the entire region of explored reduced velocities.

Our data are found to agree with the measurements of Heckman and Lindstrom[21] of π^+ and π^- stopping powers of emulsion. Using projectiles of charge plus and minus one, the Z_1^4 contribution

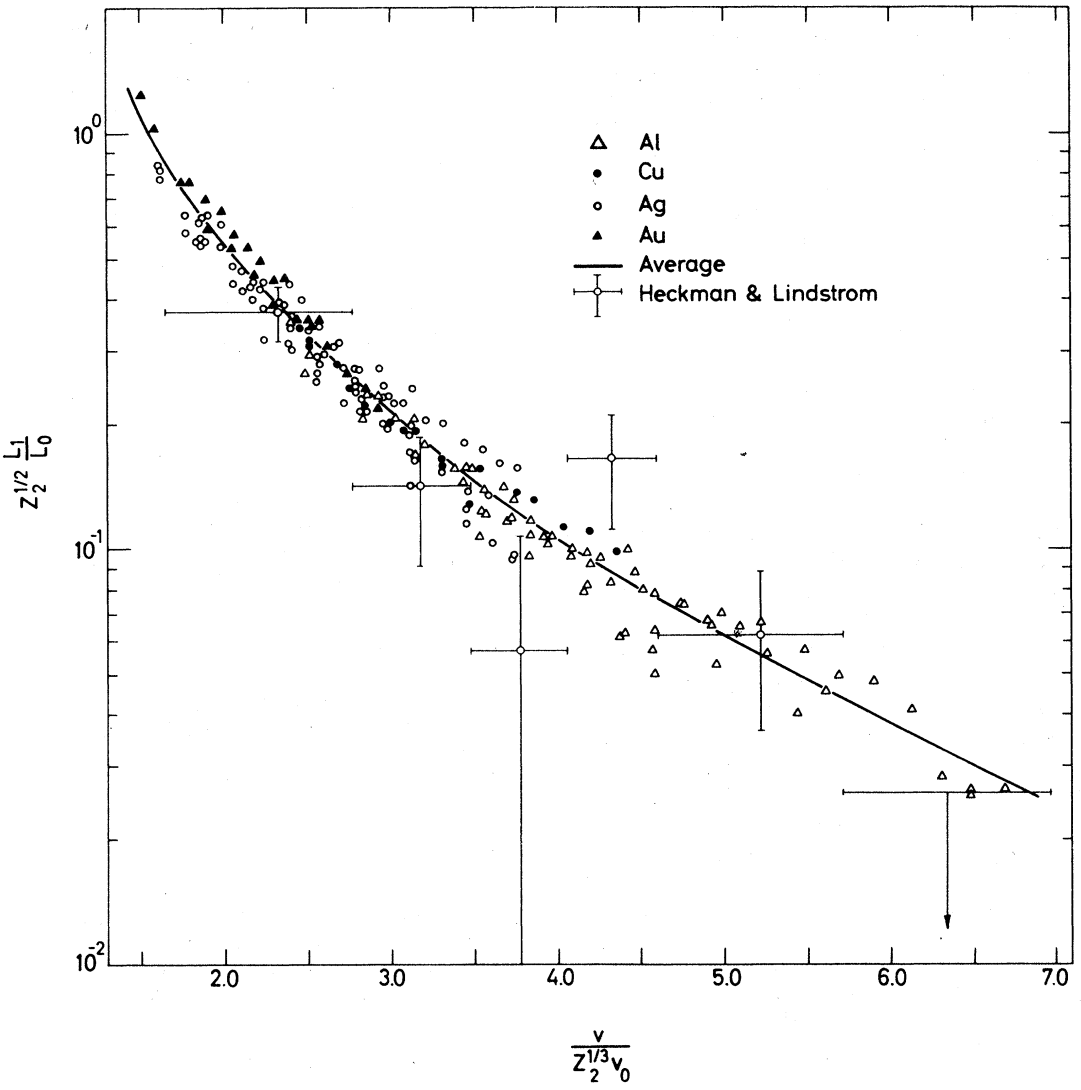

FIG. 8. Experimental values of $Z_2^{1/2}L_1/L_0$ as a function of the reduced velocity $(v/v_0)(Z_2)^{-1/3}$. The curve represents the average of the data points in the present experiment. Data from Ref. 21 are also shown.

cancels in their comparisons. Furthermore, recent stopping-power measurements[43] for hydrogen and helium in the energy range up to 600 keV/amu yield values of L_1 in good agreement with our data. Also the L_1 and L_2 values extracted from the random stopping powers for H, He, and Li ions in Au single crystals measured by Datz *et al.*[44] agree with our data. Note that Fig. 8 clearly shows that the anomalies appearing in Fig. 7 for aluminum at low projectile velocities are caused solely by inclusion of the lithium data. Similar anomalies do not appear in Fig. 8, which is independent of these data. This observation supports our interpretation, i.e., that the anomalies are caused by charge pick-up by the lithium projectiles.

C. Implications for shell corrections

According to the Bethe formula, empirical shell corrections may be determined from experimental hydrogen stopping powers as

$$(C/Z_2)' = X_H - \ln I. \tag{20}$$

This approach includes in the shell correction all deviations due to inaccuracies of the theory such as the higher-order Z_1 corrections. However, more realistic shell corrections are obtained from Eq. (14) as

$$(C/Z_2) = X_H - \ln I + L_1 + L_2. \tag{21}$$

The shell corrections obtained by Ashley[28] include

the corrections for the Z_1^3 effect of Ref. 24, but the Z_1^4 effect is not taken into account. This probably makes his shell correction too high. In Fig. 9, the shell corrections of Eq. (21) are presented together with $(C/Z_2)'$ for the energy region covered here. For L_1 and L_2, $L_0 Z_2^{-1/2}\Phi(V)$ [Eq. (18)] and Eq. (16) are used. Ashley[28] showed that the influence of the Z_1^3 term on the empirical I values is negligible. This is also the case for the Z_1^4 term. I values from Ref. 8 have therefore been used in Eqs. (20) and (21). Comparison is made to Bonderup's shell corrections,[16] $(C/Z_2)_{\mathrm{Th}}$, and the data indicate a much better accordance with theory than that obtained with $(C/Z_2)'$. Excellent agreement is found for copper and silver, while for aluminum, (C/Z_2) is larger than $(C/Z_2)_{\mathrm{Th}}$ by ~ 0.04. However, using an I value of 169 eV instead of 162 eV, which simply means a parallel shift downwards of C/Z_2 in the figure, much better agreement is found. Further, the theoretical value for gold is large compared with the experimental data at high velocities. As mentioned in Sec. IV A (see Fig. 5), our reduced stopping powers of gold are lower than most other experimental data. Hence, we are not in a position here to discern whether the discrepancy stems mainly from the calculations or from the experimental data. Note that the Risö data for gold (Fig. 5) would yield a perfect agreement with theory.

As can be seen from Fig. 9, care must be taken when existing empirical shell corrections [Eq. (20)] are used to determine stopping powers for ions different from those used in the determination of the shell corrections. In these cases, the Z_1^3 and Z_1^4 corrections must be taken properly into account.

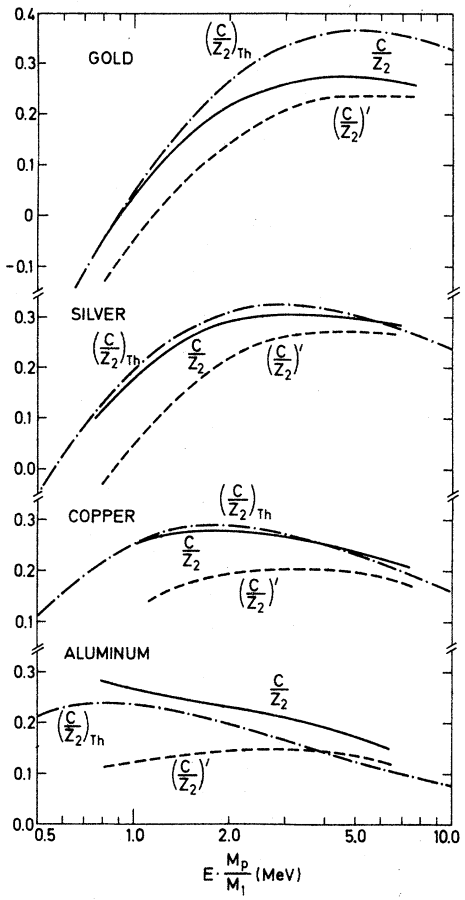

FIG. 9. Experimental shell corrections for Al, Cu, Ag, and Au obtained from Eq. (21) (fully drawn). Also shown are Eq. (20) (dotted) and the theoretical values of Ref. 16 (dot and dash) ($I_{\mathrm{Al}}=162$ eV, $I_{\mathrm{Cu}}=322$ eV, $I_{\mathrm{Ag}}=469$ eV, $I_{\mathrm{Au}}=755$ eV).

V. CONCLUSION

Stopping powers of Al, Cu, Ag, and Au for 0.8–7.2-MeV/amu hydrogen, helium, and lithium ions have been measured and found to be in agreement with the Risö data and with most other available data to within two standard deviations. The data show deviations from the dependence of the Bethe formula on projectile charge. Correction terms proportional to Z_1^3 and Z_1^4, respectively, have been extracted from the data, and they agree approximately with Lindhard's calculation of the Z_1^3 effect and Bloch's Z_1^4 correction. The scaling property of the Z_1^3 effect is found to deviate somewhat from the one described by Jackson and McCarthy. However, by using a reduced velocity $(v/v_0)Z_2^{-1/3}$ instead of $(v/v_0)Z_2^{-1/2}$ from their calculation, we found empirically a universal scaling. The Z_1^3 and Z_1^4 effects have a great influence on empirical shell corrections, and more realistic values of these have been calculated from the data. They are in good agreement with Bonderup's theoretical values.

ACKNOWLEDGMENTS

The continuous interest of J. Lindhard in the present work is gratefully acknowledged as are several discussions with E. Bonderup and H. Esbensen. Thanks are due to P. M. Petersen, who assisted in part of the measurements. A grant from the Danish State Research Foundation has supported the present work.

APPENDIX

Since the sign of the Z_1^4 effect is negative, one might suspect that part of the observed effect is due to ions not being entirely stripped of electrons, thereby interacting with a lower effective charge.

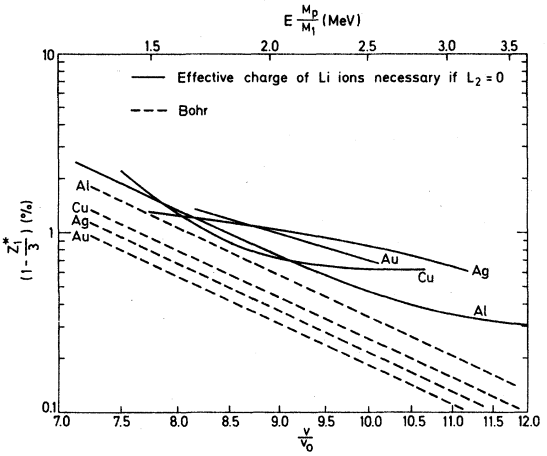

FIG. 10. Relative deviation of the effective Li charge from 3 necessary to account for the observed Z_1^4 effect (fully drawn). Theoretical curves (dotted) for the effective charge are from Eq. (23).

Such a mechanism is of no significance for hydrogen and helium ions in the energy range covered, but the effective charge of the lithium ions might be low enough to influence the results. From Bohr's capture and loss cross sections,[19] we obtain the following expression for the relative deviation of the equilibrium charge $\overline{Z}_1$ from the nuclear charge,

$$1-\frac{\overline{Z}_1}{Z_1}\sim\frac{4Z_1^5(v_0/v)^5}{Z_2^{1/3}} \tag{22}$$

valid for $v \gg v_0$. Thus the effect should be most serious in light targets. Equation (22) is in close agreement with experimental equilibrium charge states for lithium in carbon measured by Stocker and Berkowitz.[45] Since no experimental data for lithium equilibrium charges in the target materials used here are known to the authors, we used the capture and loss cross sections of Bohr to estimate the effective charge

$$Z_1^* = (\overline{Z_1^2})^{1/2}$$

of the lithium ions. If $1-\overline{Z}_1/Z_1 \ll 1$, we obtain

$$1-Z_1^*/Z_1 \sim \tfrac{5}{6}(1-\overline{Z}_1/Z_1)\,. \tag{23}$$

In Fig. 10, this expression is compared to the effective charge of lithium ions necessary to explain the observed Z_1^4 effect. It is seen that if the effect has any influence, this influence will be the larger, the lower the velocity and the lighter the target material.

[1]H. H. Andersen, A. F. Garfinkel, C. C. Hanke, and H. Sørensen, K. Dan. Vidensk. Selsk. Mat. Fys. Medd. 35, No. 4 (1966).

[2]H. H. Andersen, C. C. Hanke, H. Sørensen, and P. Vajda, Phys. Rev. 153, 338 (1967).

[3]H. H. Andersen, C. C. Hanke, H. Simonsen, and H. Sørensen, Phys. Rev. 175, 389 (1968).

[4]H. H. Andersen, H. Simonsen, H. Sørensen, and P. Vajda, Phys. Rev. 186, 372 (1969).

[5]H. Sørensen and H. H. Andersen, Phys. Rev. B 8, 1854 (1973).

[6]H. H. Andersen, H. Simonsen, and H. Sørensen, Nucl. Phys. A 125, 171 (1969).

[7]H. H. Andersen, Studies of Atomic Collisions in Solids by Means of Calorimetric Techniques, University of Aarhus, 1974 (unpublished).

[8]H. H. Andersen and J. F. Ziegler, *Hydrogen Stopping Powers and Ranges in All Elements* (Pergamon, New York, 1977).

[9]R. Ishiwari, N. Shiomi, S. Shirai, T. Ohata, and Y. Uemura, Bull. Inst. Chem. Res., Kyoto Univ. 49, 390 (1971).

[10]R, Ishiwari, N. Shiomi, Y. Mori, T. Ohata, and Y. Uemura, Bull. Inst. Chem. Res., Kyoto Univ. 45, 379 (1967).

[11]R. Ishiwari, N. Shiomi, S. Shirai, and Y. Uemura, Bull. Inst. Chem. Res., Kyoto Univ. 52, 19 (1974).

[12]H. H. Andersen, J. F. Bak, H. Knudsen, P. M. Petersen, and B. R. Nielsen, Nucl. Instrum. Methods 140, 537 (1977).

[13]H. A. Bethe, Ann. Phys. (Leipz.) 5, 325 (1930).

[14]U. Fano, Ann. Rev. Nucl. Sci. 13, 1 (1963).

[15]For a recent review of both the theoretical and experimental situation, see P. Sigmund, in *Radiation Damage Processes in Materials*, edited by C. H. S. Dupuy (Nordhoff, Leyden, 1975).

[16]E. Bonderup, K. Dan. Vidensk. Selsk. Mat. Fys. Medd. 35, No. 17 (1967).

[17]F. Bloch, Ann. Phys. (Leipz.) 16, 285 (1933).

[18]N. Bohr, Phil. Mag. 25, 10 (1913).

[19]N. Bohr, K. Dan. Vidensk. Selsk. Mat. Fys. Medd. 18, No. 8 (1948).

[20]W. H. Barkas, J. N. Dyer, and H. H. Heckman, Phys. Rev. Lett. 11, 26 (1963).

[21]H. H. Heckman and P. J. Lindstrom, Phys. Rev. Lett. 22, 871 (1969).

[22]J. C. Ashley, R. H. Ritchie, and W. Brandt, Phys. Rev. B 5, 2393 (1972).

[23]J. D. Jackson and R. L. McCarthy, Phys. Rev. B 6, 4131 (1972).

[24]J. C. Ashley, R. H. Ritchie, and W. Brandt, Phys. Rev. A 8, 2402 (1973).

[25]K. W. Hill and E. Merzbacher, Phys. Rev. A 9, 156 (1974).

[26]J. Lindhard, Nucl. Instrum. Methods 132, 1 (1976).

[27]H. Esbensen, thesis (University of Aarhus, 1977) (unpublished).

[28]J. C. Ashley, Phys. Rev. B 9, 334 (1974).

[29]H. H. Andersen, Danish AEC, Risö Report No. 93, 1965 (unpublished).

[30]F. Folkmann, K. O. Groeneveld, R. Mann, G. Nolte, S. Schumann, and R. Spohr, Z. Phys. A 275, 229 (1975).
[31]P. Tykesson, H. H. Andersen, and J. Heinemeier, IEEE Trans. Nucl. Sci. NS-23, 1104 (1976).
[32]H. H. Andersen, P. Hornshøj, L. Højsholdt-Poulsen, H. Knudsen, B. R. Nielsen, and R. Stensgaard, Nucl. Instrum. Methods 136, 119 (1976).
[33]B. R. Nielsen, thesis (University of Aarhus, 1975) (unpublished).
[34]H. Bichsel, in *Studies in Penetration of Charged Particles in Solids*, edited by U. Fano, Nat. Acad. Sci. Publ. No. 1133, Washington, D.C., 1964, p. 17.
[35]L. P. Nielsen, K. Dan. Vidensk. Selsk. Mat. Fys. Medd. 33, No. 6 (1961).
[36]E. Leminen, A. Fontell, and M. Bister, Ann. Acad. Sci. Fenn. A 6, 281 (1968).
[37]H. Nakata, Phys. Rev. B 3, 2847 (1971).
[38]A. B. Chilton, J. N. Cooper, and J. C. Harris, Phys. Rev. 93, 413 (1954).
[39]D. W. Green, J. N. Cooper, and J. C. Harris, Phys. Rev. 98, 466 (1955).
[40]C. H. Johnson and R. L. Kernell, Phys. Rev. 169, 974 (1968).
[41]H. H. Andersen, Phys. Lett. 56A, 443 (1976).
[42]H. Nakata, Can. J. Phys. 47, 2545 (1969).
[43]H. H. Andersen, F. Besenbacher, P. Hvelplund, and H. Knudsen (unpublished).
[44]S. Datz, J. Gomez del Campo, P. F. Dittner, P. D. Miller, and J. A. Biggerstaff, Phys. Rev. Lett. 38, 1145 (1977).
[45]H. Stocker and E. H. Berkowitz, Can. J. Phys. 49, 480 (1971).